Suppression of photorefractive damage with aid of steady-state temperature gradient in nominally pure LiNbO3 crystals

Sergey M. Kostritskii, Oleg G. Sevostyanov, Michel Aillerie, Patrice Bourson

Suppression of photorefractive damage with aid of steady-state temperature gradient in nominally pure $LiNbO_3$ crystals

S. M. Kostritskii,[1] O. G. Sevostyanov,[2] M. Aillerie,[3,a)] and P. Bourson[3]
[1]*MPTE Department, Moscow Institute of Electronic Technology, Moscow, 124498 Zelenograd, Russia*
[2]*Physics Department, Kemerovo State University, 650043 Kemerovo, Russia*
[3]*Laboratoire Matériaux Optiques, Photonique et Systèmes, University Paul Verlaine of Metz and Supélec, UMR CNRS 7132, 2 Rue E. Belin, 57070 Metz, France*

(Received 10 July 2008; accepted 19 October 2008; published online 4 December 2008)

Photorefractive damage (PRD) in as-grown, oxidized, and slightly reduced nominally pure $LiNbO_3$, and iron-doped crystals with different compositions has been studied with the closed-aperture *Z*-scan and pseudo-*Z*-scan techniques at uniform temperature distribution, as well as at a steady-state temperature gradient ∇T, created by two external thermoelectric elements in the transverse direction to the light beam trajectory. The most important experimental finding consists of the demonstration of the possibility of a full PRD suppression in nominally pure crystals with the aid of a relatively small temperature gradient (12.5–84 K/cm), if ∇T is above a threshold value specific for each crystal studied. The threshold ∇T_{th} decreases significantly with the increase in the so-called bipolaron absorption band (center at 470–500 nm) in the optical spectra, and it is not correlated with the composition of the crystals within the studied range of compositions ($[Li]/[Nb]=0.946-0.983$). No any partial suppression of PRD was observed in iron-doped ($[Fe] \geq 0.01$ wt %) lithium niobate crystals, even at the largest temperature gradient (85 K/cm) used in our study. To explain these experimental results, we use theoretical model taking into account local changes of spontaneous polarization (i.e., polarization charge field) at photoionization of intrinsic defects (polarons, bipolarons, and hole polarons). It has been shown that a steady-state temperature gradient may induce a local thermoelectric current of light-induced charge carriers and their instant recombination, resulting in a decrease in the polarization space-charge field and hence, a light-induced refractive index change. The latter mechanism may induce the full PRD suppression, if macroscopic charge separation (space-charge field effect) gives insignificant contribution to the total light-induced electric field, as in as-grown and reduced nominally pure $LiNbO_3$ crystals. © *2008 American Institute of Physics*. [DOI: 10.1063/1.3035948]

I. INTRODUCTION

The photorefractive damage (PRD) is the most dramatic problem for lithium niobate crystal applications in electro-optic and nonlinear optic devices utilizing high-intensity laser beams. To suppress this parasitic effect, a large variety of methods has been developed: crystal doping with so-called optical damage-resistant impurities,[1–3] stoichiometry control,[4,5] hydrogen implantation,[6] heating up to 180–230 °C,[7] and application of external electric field.[8] However, some of these methods are expensive and other ones do not provide stable appropriate results. At the same time, very promising results have been obtained with inhomogeneous temperature field caused by strong absorption of high-intensity laser beams in iron-doped $LiNbO_3$ (LN) crystals.[9,10] However, the PRD variations with time have sophisticated nonreproducible character due to the dependence of temperature profile on exposure time and many external conditions.[9] Note that this effect has not been studied yet in nominally pure crystals because of relatively small optical absorption. Therefore, we propose to use the following approach: The stationary nonuniform temperature profile (steady-state temperature gradient) is produced by a system of external heaters and/or coolers, e.g., two thermoelectric (Peltier) elements at the opposite sides of sample studied. According to the previous studies,[9–11] the very strong variations of PRD magnitude should be expected even at relatively small values of temperature gradient. Until yet, the photorefractive (PR) effect has been studied in some detail for equilibrium temperature conditions when the warm up of the whole volume of the polar sample is uniform. However far less information is available on the behavior of PR crystals in nonequlibrium thermal conditions when a temperature gradient exists. Thus, investigation of such a behavior of PR properties, including PRD, is actual task with fundamental point of view, too.

In this paper we report about experimental and theoretical study on influence of steady-state temperature gradient on PRD effect in nominally pure LN crystals. Also, we check possibility for significant suppression of the PRD in bulk LN elements used in real electro-optic and nonlinear optic devices.

II. EXPERIMENTAL

To study PRD quantitatively, we used the closed-aperture *Z*-scan (CAZ) technique,[12] as well as the pseudo-*Z*-scan technique, when measurements of transmitted

a)Electronic mail: aillerie@metz.supelec.fr.

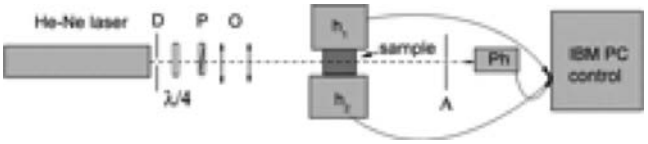

FIG. 1. Setup for study of PRD suppression by temperature gradient: *D* is diaphragm; λ/4 is quarter-wave plate, *P* is polarizer; *O* is twin lenses objective ($f=150$ mm); h_1 and h_2 are thermoelectric elements (h_1 is heater, h_2 is the Peltier element); *A* and Ph are small aperture diaphragm and photodiode respectively, located in the far field region.

intensity are realized at a fixed postfocal position of the samples.[13,14] The radiation of a He–Ne laser (632.8 nm) is used with various laser beam powers ranged from 2.5 to 28 mW. A polarizer is used to obtain exact extraordinary polarization of light in the studied crystal. Therefore, the effective light power injected into the crystal was ranged from 1.1 to 12.3 mW.

The *Z*-scan technique is a well-established sensitive method to determine nonlinearities of optical materials. The experimental arrangement corresponding to this technique is represented in Fig. 1. Without a pinhole between the sample and the photodiode, the open-aperture *Z*-scan scheme allows obtaining the nonlinear absorption coefficients while with a pinhole, the CAZ scheme allows determining the sign and the magnitude of the nonlinear refractive index. With this arrangement, we can also determine the degree of the PR nonlinearity of PR crystals. In our optical setup, a laser beam is focused by a lens with a focal length of 150 mm. The investigated samples are moved by a translation stage for a variable number of the fixed steps (step length is 0.5 mm) along the *Z* axis of the setup through the focal point of the focusing lens. Such an arrangement allows to measure the dependence of the transmittance on crystal positions relative to the focal point, i.e., so-called the *Z*-scan trace.[14,15] Each sequent measurement procedure is performed for an optically undamaged crystal area. To obtain it, the crystal is translated for 0.2 mm in direction perpendicular to plane of Fig. 1. A diaphragm with 0.5 mm aperture transmitting 3% of laser radiation is fixed at distance of 350 cm from the focal plane in the closed-aperture scheme. The photodiode, followed by a digital voltmeter was kept behind this aperture for intensity measurements of the output radiation.

In order to evaluate the PRD magnitude, i.e., the steady-state value Δn_s, the light-induced trajectory changes in an extraordinarily polarized laser beam due to PR defocusing, have been studied with the pseudo-*Z*-scan technique. The intensity distributions (shape and magnitude) at the focus and at a long distance after crystal were recorded with the aid of closed-aperture photodiode within the same manner as in *Z*-scan study. It is known[13] in fact, that such investigation allows measuring the photorefraction with reliable precision. We have used a simple model[4] for evaluation of Δn_s from the laser beam trajectory: $\Delta n_s = 4n_e\{(y/y_o)-1\}/(x/y_o)^2$, where n_e is the extraordinary refractive index, x is the path length of the laser beam in the sample, y is the radius of the laser spot at half intensity in steady state, and y_o is the radius of the laser spot at half intensity in initial state (at exposition time $t=0$).

The nonlinear absorption of the samples was examined by open-aperture measurements as well. To study the intensity dependence of the nonlinear absorption, we used calibrated neutral density filters in range of *D* from 0.5 to 2.3.

We measured the PR nonlinearity and PRD magnitude of LN crystals with thickness *h*, i.e., $x=h$, varying from 5 to 8 mm. Nominally pure lithium niobate crystals with different compositions were used in our investigation: as-grown samples (2–5, Table I), samples chemically reduced by annealing in vacuum (10^{-3} Torr at 500 °C, samples 6 and 7), or in hydrogen atmosphere at 500 °C for 0.5–11 h and one sample deeply oxidized (sample 1, Table I) fabricated by annealing of an as-grown sample at 1000 °C for 15 h in pure oxygen atmosphere.

The optical transmission of the samples was measured using polarized light at normal incidence on a SF-2000 spectrometer in the wavelength range 0.2–1.1 μm. The surrounding medium was air, and all measurements were done at room temperature. The use of a difference spectroscopy method enabled us to resolve the absorption bands connected with the intrinsic defects and impurities. It should be noted that all the samples studied (see Table I) show a weak additional absorption band (with values from 0.02 up to 0.154 cm^{-1}) for $\lambda \geq 330$ nm extending up to 700 nm. Additional chemical reduction via annealing in vacuum or H_2 atmosphere has been established to introduce a large amount of this additional absorption. This absorption growth correlates closely with a significant increase of the so-called bipolaron absorption band,[1,4,16] centered at 470–500 nm. Thus, the additional absorption presumably corresponds to this large concentration of bipolarons in annealed crystals and, according to the previous data,[4,5,17] we can conclude that the weak additional absorption in as-grown crystals is caused mainly by the bipolaron absorption band and any nominally

TABLE I. Parameters of lithium niobate samples used in our PRD experiments.

	Sample No.						
	1	2	3	4	5	6	7
Optical absorption coefficient $\alpha(\lambda=470$ nm) (cm^{-1})	0.022	0.078	0.09	0.092	0.099	0.117	0.154
Optical absorption coefficient α' ($\lambda=470$ nm) (cm^{-1})	<0.003	0.006	0.007	0.009	0.015	0.032	0.063
[Li]/[Nb] ratio	0.950	0.983	0.946	0.950	0.973	0.967	0.962

pure lithium niobate can be regarded as a weakly reduced crystal with marked concentration of bipolarons.

The optical absorption coefficient α was calculated from the transmission data by the following equation using the Newton–Ralphson method

$$T\{[n(n+2)(n+1)^2+(1+4n+2n^2)k^2+k^4]\exp(4\pi kd/\lambda) + [n(n-2)(n-1)^2+(1-4n+2n^2)k^2 + k^4]\exp(-4\pi kd/\lambda)\} - 16(n^2+k^2) = 0, \quad (1)$$

where T is the optical transmission, n is the extraordinary refractive index, d is the thickness of the sample, λ is the wavelength of the incident light, and k is the extinction coefficient which is related to α by

$$\alpha = 4\pi k/\lambda. \quad (2)$$

Mathematical fitting of the spectral dependence of α was used to extract contributions of long-wavelength tail of fundamental absorption and light scattering and to evaluate the true additional absorption related to bipolarons (mainly) and extrinsic defects (secondary). The values of this additional absorption coefficient calculated with aid of such a fitting are denoted in Table I as α'. The samples characterized in this study are presented in Table I with their linear absorption coefficients α and α', stoichiometric composition, and geometric dimensions.

The two thermoelectric Peltier elements in the *Z*-scan setup are used to produce a well-controlled value of steady-state temperature gradient in the crystal under study, Fig. 1. One of these elements is the thermoelectric heater operating in the 20–80 °C range and the second one is the thermoelectric cooler, allowing to provide a constant and fixed temperature of the bottom part of the crystal within the 12–23 °C range. The light beam inducing PRD propagates in the perpendicular direction to the temperature gradient vector.

The two crystals among samples studied optically were prepared for direct pyroelectric measurement. The 200-nm-thick Al electrodes were deposited on +C and −C surfaces, and connected by an Al wire. When the temperature of the sample is constant, no current flows through the circuit. However a temperature increase causes a net dipole moment and, consequently, a decrease in the spontaneous polarization. The quantity of bound charge then decreases, as it is compensated by the redistribution of free charges, which induces the pyroelectric current in the circuit. If the sample had been cooled instead of heated, the current's sign would be reversed. In an open circuit, the free charges would simply remain on the electrodes and a voltage could be measured.

III. EXPERIMENTAL RESULTS

To compare PRD magnitudes obtained at different temperature gradients, we used the pseudo-*Z*-scan arrangement, and we recorded the temporal evolution of the transmitted intensity J in a fixed (postfocal) crystal position. Normalized to the input intensity, we define three thresholds that occur at different times during experiment: J_1 and J_3 are the initial and saturation values of the output intensities in the PRD process, while J_2 is the saturation value after the thermal gradient is applied onto the sample. We report in Fig. 2 for the as-grown sample the time dependence of the transmitted intensity J normalized to its input value for two different experimental conditions. Corresponding to a time delay equal to 16 min, the left part of Fig. 2 shows the transmitted intensity J as measured with an extraordinary polarized laser beam at room temperature. The laser beam power used for this experiment is adjust at 12 mW. Time constants are determined from computer fitting of the experimental curves to the function of $J(t)=J_3+(1-J_3)\exp(-t/\tau)$. We have compared the transmittance in the stationary state (J_3) obtained with various crystals (not represented), which allowed us to state some findings in the PR properties. The rise time τ of PRD is shortest for chemically reduced LN, and it is shorter for as-grown than for oxidized LN as well. It has been found also that the time constant is inversely proportional to the light intensity used for experiments and to the optical absorption coefficient of crystals, and it is directly linked to impurities concentration. However, among chemically reduced crystals, the sample with highest optical absorption coefficient has the largest J_3 and the shortest τ. The difference between transmitted intensities J_1 and J_3 has been used as a rough qualitative measure of PRD magnitude,[4] as well as input data for evaluation of steady-state refractive index change Δn_s caused by PR effect, Table II. PRD in the as-grown and oxidized LN crystals is more significant in comparison with those in chemically reduced samples. Note, that PRD becomes undetectable with our experimental method in reduced crystals annealed for more than 1 h.

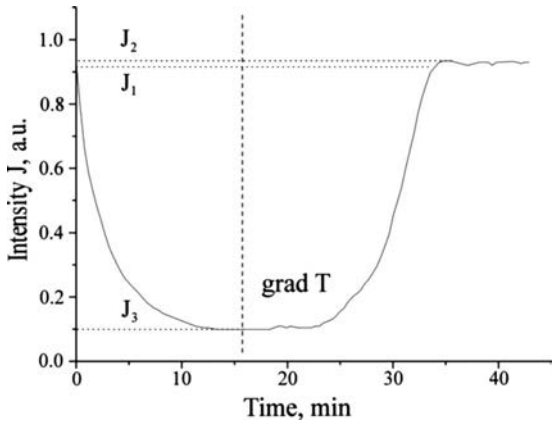

FIG. 2. PR response for as-grown sample 4 (see Table I) at room temperature (time period from 0 to 16 min), at transient state during heat-up of crystal's top part (time period from 16 to 19 min) and at steady-state temperature gradient $\nabla T=41.6$ °C/cm (period from 19 to 45 min).

The most important experimental finding of this study consists of qualitative and quantitative experimental proofs of the possibility of a full suppression of PRD with aid of steady-state temperature gradient applied in direction perpendicular to laser beam propagation. For example, the right part of Fig. 2 shows the temporal evolution of transmitted intensity, when steady-state gradient ($\nabla T \approx 41.6$ °C/cm) is applied by the thermoelectric elements with $T_{h1}=45$ °C and $T_{h2}=20$ °C to the crystal 4 (see Table II) with a 6 mm thickness along the gradient direction. Note that we use a fast constant-rate gradual change in T_{h1} with heating rate of 10 °C/min from room temperature to a target temperature.

TABLE II. PRD magnitude Δn_s^0 at $\nabla T=0$ and parameters (∇T_{th} and SF) of the PRD suppression effect in different samples.

	Sample No.						
	1	2	3	4	5	6	7
$\Delta n_s^0 \times 10^{-4}$	1.3	0.7	1.6	0.9	1.1	0.9	0.85
∇T_{th} (K/cm)	84	40	41	37	32	18.0	12.5
SF at grad $T=5$ K/cm	0.03	0.19	0.12	0.33	0.25	0.35	0.36
SF at grad $T=15$ K/cm	0.17	0.53	0.38	0.72	0.69	0.83	1.0
SF at grad $T=25$ K/cm	0.31	0.86	0.73	0.91	0.95	1.0	1.0

Therefore, for the case shown in Fig. 2, the steady-state gradient was developed before beginning of the output intensity recovery. At the same time, homogeneous heating of any LN samples induces only small changes in the steady-state PRD magnitude, as the maximum temperature used in our study was small (80 °C) relatively to the well-known data[7–11] on temperature dependence of PRD magnitude.

The total suppression of PRD, i.e., when $J_2=J_1$ can be observed, if the temperature gradient is equal or above a certain threshold value ∇T_{th}. As ∇T_{th} depends on crystal parameters, this threshold value has different magnitudes for crystals studied, and varies within the range from 12.5 to 85.5 °C/cm for as-grown and slightly reduced (with annealing time $\leq$0.67 h) nominally pure crystals. The different magnitudes of temperature gradient were obtained by variation of temperature T_{h1} of one thermoelectric element (see Fig. 1) within the 20–80 °C range at a fixed temperature set at $T_{h2}=20$ °C for the second thermoelectric element. The final level of the output intensity J_2 reached at steady-state gradient is insignificantly larger than J_1 ($\leq$5%), as PRD does not reach a true saturated state in the initial stage of our experiment (left part of Fig. 2). To reach such a state, more longer exposure is required in the initial stage within levels of light intensities used in our experiments, that is nonconvenient practically and the quasisaturated state reached is sufficient for our investigation.

At temperature gradients smaller than the threshold value ∇T_{th} required for full suppression of PRD, recovery of the output intensity is not observed (Fig. 3), but instead of it, a marked increase in the output intensity is observed with $J_2 \ll J_1$, i.e., with a partial suppression of PRD. In this case, residual part of PRD decreases almost proportionally to ∇T, when this latter is significantly smaller (by a factor $\geq$25%), than the temperature gradient threshold ∇T_{th}. The partial suppression of PRD can be characterized by a suppression factor (SF) defined as $SF(\nabla T)=1-\Delta n_s(\nabla T)/\Delta n_s(\nabla T=0)$. If ∇T increases in the range near this threshold, a sharp decrease in residual PRD is observed and SF approaches to 1. At temperature gradients above the critical value, the total suppression of PRD is observed and evaluation of PR effect magnitude from distortion of light beam trajectory gives $\Delta n_s=0$ (i.e., SF=1). These observations, for a given sample at fixed light-intensity value, are done independently of the initial ∇T and average temperature. Comparison of the partial PRD suppression effect in different crystals demonstrates clearly that changes in SF correlate with changes in optical absorption coefficient α', see Tables I and II.

At any fixed temperature gradient $\nabla T<\nabla T_{th}$, chosen in accordance with the ∇T_{th} for a given crystal, attenuation of the output laser power, obtained with the aid of the optical arrangement composed of a quarter-wave plate and polarizer (see Fig. 1), provides a sharp decrease in the normalized difference between output intensities J_2 and J_1, i.e., the partial PRD suppression, described by the relative parameter SF, becomes to be more significant. Besides, for any crystals studied, specific parameter of ∇T_{th} decreases with the decrease in light beam intensity within the crystal.

It is very important to note that in iron-doped ([Fe] $\geq$0.01 wt %) lithium niobate crystals, any partial suppression of PRD was not observed even at the largest temperature gradient of 85.5 K/cm used in our studies. In these crystals PRD is much stronger in comparison with any nominally pure crystal. In fact, PR defocusing of laser beam is much significant and, therefore, steady-state value of output intensity detected by closed-aperture photodiode in a fixed postfocal point is very small and it is not affected by steady-state temperature gradient. There is only fast quasichaotic transient change in the output intensity during heating and cooling processes, when temperature distribution across crystal demonstrates significant temporal changes and, thus, steady-state temperature gradient is not developed yet. Such a fast transient change is observed also in all nominally pure crystals and, according to previous studies,[7,9,10] it may be attributed to the influence of thermo-optic and pyroelectric effects.

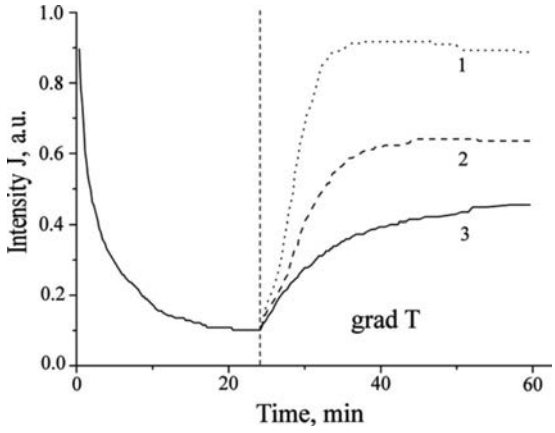

FIG. 3. Kinetics of PR response at various temperature gradients ∇T: $\nabla T_1 > \nabla T_2 > \nabla T_3$ (curves 1, 2, and 3, respectively). These data have been obtained at $\nabla T_1=13.3$ °C/cm ($T_{h2}=20$ °C and $T_{h1}=28$ °C) with sample 7, having minimum threshold value of stationary gradient ($\nabla T_{th}=12.5$ °C/cm, see Table II) required for the full suppression of PRD.

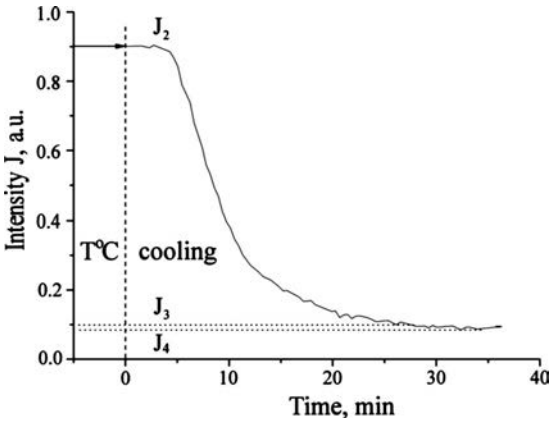

FIG. 4. Kinetics of output intensity induced by PRD recovery in sample 4, when temperature gradient is removed because of the sharply decrease in the thermoelectric element temperature T_{h1}. The final stage of this experiment is a steady-state uniform temperature field ($T_{h1}=T_{h2}=$const), which is reached in 7 min after switching off the thermoelectric element h_1, as temperature gradient decreases down to zero during this period. Experimental conditions are the same with Fig. 2, and ordinate $t=0$ in this figure corresponds to ordinate $t=45$ min in Fig. 2.

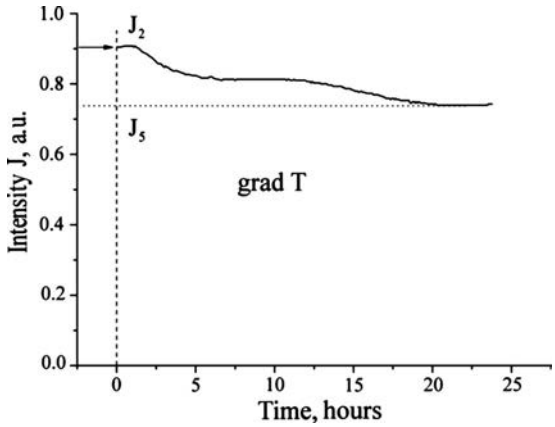

FIG. 5. Long-term drift of the output intensity after initial full suppression of PRD with aid of stationary temperature gradient in nominally pure as-grown lithium niobate crystal (sample 4). The experimental conditions are the same than in Fig. 2, and ordinate $t=0$ in this figure corresponds to ordinate $t=45$ min in Fig. 2.

In any iron-doped and undoped crystals this transient intensity change is most significant, when heater and cooler (Peltier's elements h_1 and h_2, Fig. 1) are applied to $+Z$ and $-Z$ surfaces of crystal, i.e., the polar crystal axis (Z axis) is directed along a virtual line passing through heater and cooler.

This phenomenon of PRD suppression is completely reversible. For example, Fig. 4 shows temporal evolution of output intensity, when a steady-state temperature gradient field is removed by cooling down the sample with the thermoelectric element h_1 to the final state $T_{h1}=T_{h2}=20$ °C. Full recovery of PRD magnitude is observed, i.e., the steady-state value of light-induced refractive index change Δn_s reaches its initial value (developed before application of ∇T), when temperature gradient completely disappears. Such a suppression/recovery cycle may be repeated unlimited number of times. Some small differences between output intensities J_3 and J_4 (see Figs. 2 and 4) are observed only when the steady-state value of PRD is not reached before application of temperature gradient ∇T.

It has been established that the same suppression of PRD may be induced by temperature gradient field created by Peltier cooler h_2, if $T_{h2}<T_{h1}$ and T_{h1} is some stable temperature near (or equal) the room temperature (see Table III). In this case, it is possible to reach the full PRD suppression with some extra efforts to escape water vapor condensation on crystal surface, as values of T_{h2} required for all the samples studied are below a dew point for air at standard surrounding conditions.

It is of note that the dominating part of PRD, as considered in this study, corresponds to the short-time contribution of a general drift that occurs in long-exposure experiments in LN crystals (or LN based devices). As shown in Fig. 5 for the as-grown sample 6, after full suppression of PRD in the short-time range (time below 2 h), some small PRD appears in the long-time exposure range. The specific time of buildup of this small PRD is much longer in comparison with the PRD kinetics existing for crystal that is not placed in a temperature gradient field. Comparing Fig. 2 and 5, this specific time difference is found to be two orders of magnitude. Same qualitative behavior at long-term exposure is observed in all other nominally pure samples under temperature gradient field.

TABLE III. Dependence of SF on temperature gradient, created by cooling down of bottom part of a crystal via Peltier element h_2 (see Fig. 1).

Sample No.	grad $T=3.4$ K/cm	grad $T=7.2$ K/cm	grad $T=13.3$ K/cm
1	≤0.02	0.03	0.15
4	0.23	0.38	0.65

If the stationary temperature gradient is developed across crystal before illumination, the same long-term drift of the output intensity (see Fig. 5) is observed. However, in this case its initial value is equal to J_1 (see notification given in Fig. 2). Therefore, with practical point of view, the temperature gradient allows to decrease significantly PRD in nominally pure lithium niobate crystals, but full suppression of PRD is not available for stable long-term operation. Despite this drawback, the partial suppression of PRD via temperature gradient has great practical importance, as inherent residual PRD is smaller than maximum acceptable levels required in many applications.[7] Main advantages of this novel method of PRD suppression consist of its relative technical simplicity and of its possibility to select any operational or functioning temperature value within a local area, e.g., within waist of focused laser beam. The latter is one of the most important tasks for nonlinear optical converters, where an exact phase matching is necessary.

It has been found that this PRD suppression effect is possible only under the combined influence of temperature gradient and illumination, Fig. 6. The very slow dark relaxation of PRD (specific time has order of several tens of hours) in all lithium niobate crystals is observed without illumination at any temperature gradient in the studied range. The small difference in dark relaxation kinetics between cases of temperature gradient and uniform room temperature may be related to the pyroelectric effect and to the dark

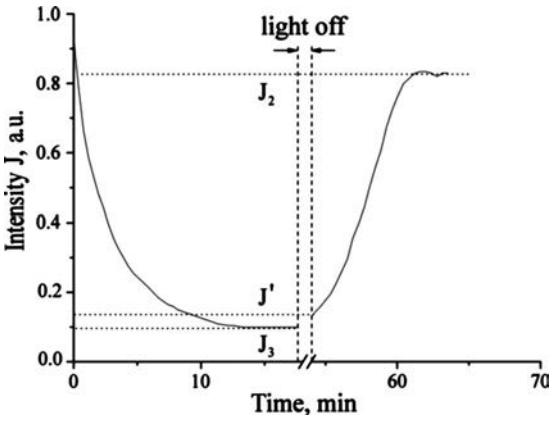

FIG. 6. Suppression of PRD effect (time period from 53.5 to 63 min) delayed by dark relaxation (time period from 17.5 to 53.5 min) of PRD in sample 4 at stationary temperature gradient ($\nabla T = 41.6\ ^\circ\mathrm{C/cm}$) applied within time period from 21.5 to 63 min. PRD is induced at room temperature (i.e., at $\nabla T = 0$) during period from 0 to 17.5 min, and steady-state ∇T value is reached after period from 17.5 to 21.5 min.

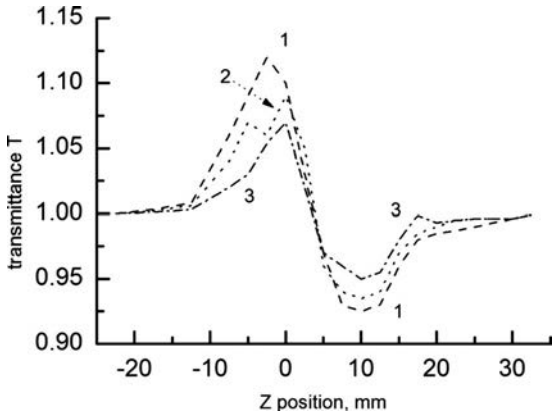

FIG. 8. *Z*-scan traces of nominally pure sample 7 at stationary room temperature (1) and with different steady-state gradients—3.8 °C/cm (2) and 6.6 °C/cm (3). The light intensity is around 0.8 $\mathrm{kW/cm^2}$.

conductivity growth due to an increase of the average temperature. Simultaneously, these data clearly show that pyroelectric effect cannot be regarded as dominating mechanism of the PRD suppression effect reported in this paper.

In order to compare quantitatively the PR nonlinearity changes in different samples under influence of the variable temperature gradient, we performed *Z*-scan measurements under same experimental conditions, i.e., using the same optical and thermal arrangements with a He–Ne laser at 10 mW output power. As Fig. 7 shows in the slightly reduced nominally pure lithium niobate sample 7 (see Table I), the CAZ traces are opposite in sign for measurements with and without the steady-state gradient of 14 °C/cm. This temperature gradient is created by the heater h_1, keeping the constant temperature of 23 °C for top side of the sample, and Peltier element h_2, cooling the bottom side for stable temperature of 14.6 °C.

For all measurements performed at room temperature in absence of temperature gradient, we have observed shape of *Z*-scan trace, which is typical for the negative refraction index change, as shown by trace 1 in Fig. 7. According to previous studies,[12–15] it shows clearly that the PR effect gives the dominating contribution to the integral nonlinear response. In case of steady-state temperature gradient, the

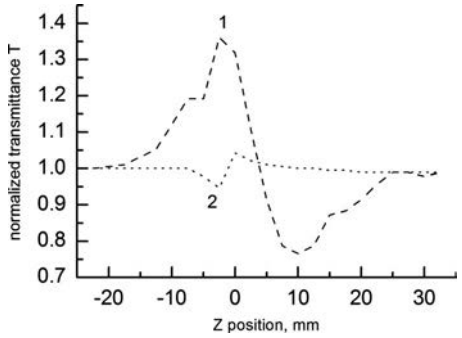

FIG. 7. *Z*-scan traces of nominally pure sample 7 at stationary room temperature (1) and with a steady-state gradient equal to 14 °C/cm (2). The light intensity is around 2.5 $\mathrm{kW/cm^2}$.

Z-scan trace changes quantitatively and qualitatively, depending on gradient values: At small and moderate ∇T, the sequence order of peak and valley in *Z*-scan trace, i.e., the so-called negative sign of *Z*-scan traces,[13] does not change with temperature gradient, but for larger ∇T ($\nabla T > \nabla T_{\mathrm{th}}$), as plotted by trace 2 in Fig. 7, there is an alteration of the sign of the *Z*-scan trace, i.e., the modulation of the *Z*-scan trace should be characterized by the so-called positive sign.[13,14]

As we can see in Fig. 8, demonstrating only cases of negative modulation of the *Z*-scan trace within our experimental conditions, larger is ∇T, smaller is the contrast between peak and valley in the *Z*-scan traces. It means that the nonlinear optical refraction is significantly smaller in the case of temperature gradient, than for homogeneous temperature distribution. According to our experimental study, the key result is the presence of a consequent peak-valley contrast in the *Z*-scan trace at stationary uniform temperature ($\nabla T = 0$) and a decrease, down to a quasiescape of the peak-valley contrast with the increase in the temperature gradient ∇T. A specific temperature gradient, ∇T_{sp}, of such a quasiescape is different for different nominally pure lithium niobate crystals and the various ∇T_{sp} coincide roughly with data on ∇T_{th} in different crystals. Note that measurement accuracy of ∇T_{sp} is much lower than of ∇T_{th}. In all the cases of large temperature gradient ($\nabla T > \nabla T_{\mathrm{sp}} \approx \nabla T_{\mathrm{th}}$), modulation sign of *Z*-scan trace is positive and modulation depth, i.e., contrast between peak and valley, is much smaller than at small and moderate values of ∇T, Figs. 7 and 9. The modulation depth depends on light intensity in all undoped crystals. Therefore, we can assume that application of a high-power laser, e.g., $\mathrm{Ar^+}$-ion one weighted by the influence of the wavelength, should provide a significant modulation depth of *Z*-scan trace even at large ∇T, when modulation has positive sign and, according to Ref. 5, may be explained clearly by thermo-optic effect.

Finally, there is a clear correlation between the PRD magnitude and modulation depth of the corresponding *Z*-scan trace at comparison of either the different samples at fixed values of ∇T, or data obtained at different ∇T for a given crystals. Thus, *Z*-scan measurements can be used as well to compare the PRD suppression effect in different crys-

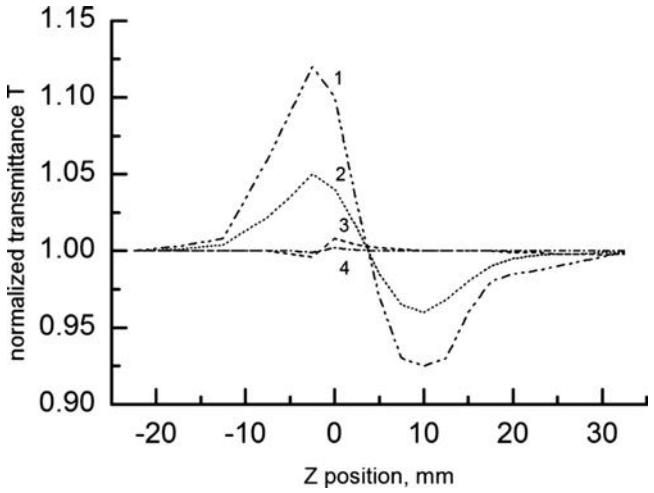

FIG. 9. *Z*-scan traces of nominally pure sample 7 at stationary room temperature (curves 1 and 2) and with a steady-state gradient equal to 14 °C/cm (curves 3 and 4 traced near $T=1$). The light intensity is around 0.8 kW/cm^2 (1, 3) and 0.3 kW/cm^2 (2, 4).

tals since the peak-valley configuration distinguishes clearly samples above and below the threshold value of ∇T, which is a specific parameter for each crystal.

IV. DISCUSSION

To explain the origin of the PRD suppression effect with temperature gradient in lithium niobate crystals, we consider at first the common mechanisms discussed previously: pyroelectric effect,[9,10] change in dark and photoconductivity with temperature,[7,8] and thermoelectric current excitation caused by photoinduced carriers diffusion directed by temperature gradient along the gradient vector.[11]

The pyroelectric effect can influence PRD due to the appearance of a strong pyroelectric field. It has been demonstrated[9,10] that macroscopic charge separation due to pyroelectricity represents an important contribution to PRD in ferroelectrics, which can occur whenever the temperature is raised significantly (e.g., $\Delta T \geq 32$ K for LN).[9] Nevertheless it is to be of note that the strong pyroelectric effect is only observable during and shortly after the period in which the temperature changes[7,9] and the specific time of this transient phenomenon is much shorter in comparison with the effects reported here (see Figs. 2 and 5). The steady-state pyroelectric field can be created by stationary temperature gradient, but it has smaller magnitude. However at certain conditions,[11] this field can compensate totally the light-induced space-charge field, creating the PRD suppression. The pyroelectric field E_{pyro} and pyroelectric current i_{pyro} are expressed by

$$E_{\text{pyro}} = \gamma \Delta T/(\varepsilon - 1)\varepsilon_0 = [1/(\varepsilon - 1)\varepsilon_0](\nabla T d)\gamma,$$

$$i_{\text{pyro}} = [\sigma/(\varepsilon - 1)\varepsilon_0]\Delta T \gamma, \tag{3}$$

where $\gamma = -\partial P_s/\partial T$ is the pyroelectric coefficient, P_s is the spontaneous polarization, ε is the static dielectric permittivity, ε_0 is the dielectric constant, σ is the electric conductivity, and d is the laser beam diameter.

In case of nominally pure congruent lithium niobate crystals, the values of γ and ε_{33} (static dielectric permittivity along the optical axis) are equal to

$$\gamma = -\left(\frac{\partial P_s}{\partial T}\right) = 8.3 \times 10^{-5} \text{ C/m}^2 \text{ K}, \quad \varepsilon_{33} = 28.$$

Hence, as calculated with the previous values, the pyroelectric field created by the temperature gradient $\nabla T \approx 12.5$ K/cm induced in sample 7 (see Fig. 3 and Table I) corresponds to $E_{\text{pyro}} \approx 0.42 \times 10^3$ V/cm. It is not sufficient even for a significant partial suppression of PRD because this value is much smaller than light-induced space-charge field E_{sc} responsible for PRD, which is estimated to be around 15 kV/cm in our experimental conditions.[4] Moreover, it has been established[11] that temperature gradients equal or greater than 10^3 K/cm are able to eliminate the strong PRD, which is generated by the light-induced space-charge field E_{sc} of order of magnitude in the range of 40–100 kV/cm in iron-doped samples at low and moderate light intensities. Temperature gradients less than 500 K/cm have no observable effect upon the strong PRD observed in iron-doped lithium niobate.[11] During our experiments, the maximum temperature gradient value used is equal to 85.5 K/cm, as it is sufficient for total suppression of PRD in any undoped LN sample studied. By the way, even this largest gradient is sufficient, according to Ref. 11, to suppress the PRD induced by $E_{\text{sc}} \leq 3$ kV/cm, i.e., optical damage caused by birefringence variation of order 10^{-5}. However, such a value of optical damage cannot induce both the strong PR defocusing, Figs. 2 and 6 and marked perturbation of *Z*-scan traces, Figs. 7 and 9 experimentally observed. Thus, the steady-state pyroelectric effect cannot be regarded as the dominating mechanism of PRD suppression in lithium niobate crystals.

In our experiments the change of dark and photoconductivity that would be induced by temperature gradients cannot give any significant contribution in PRD magnitude variation. Indeed, the maximum temperature used in our study was relatively low (80 °C), according to the well-known relation between the decrease of light-induced space-charge field and the growth of electric conductivity at high temperatures,[7] where almost full suppression of PRD was observed at homogeneous heating for the temperatures above 140 °C only.[7,8]

Nonequlibrium thermal conditions, when a temperature gradient produced by nonuniform crystal heating/cooling, give rise to an intensive heat flux. According to the data on light-induced charges transport in lithium niobate crystal,[11] the strong thermoelectric current component parallel to the gradient vector should appear within illuminated area, providing a consequent extra contribution in light-induced space-charge field.

To include the thermoelectric effect in our consideration, we add an extra term j_{diff} in the equation describing the light-induced current j. This term j_{diff} is related to the diffusion of photoexcited electric carriers. Thus, PR effect is assumed to be caused only by macroscopic space-charge field due to the light-induced current j, which consists of three terms:

$$j = j_{\mathrm{pv}} + j_{\mathrm{drift}} + j_{\mathrm{diff}}, \tag{4}$$

i.e.,

$$j = \beta_{ijk} e_j e^*_k I + \sigma E_{\mathrm{sc}} + k_B T\left(\mu_n \frac{\partial n}{\partial z} + \mu_p \frac{\partial p}{\partial z}\right), \tag{5}$$

where j_{pv}, j_{drift}, and j_{diff} are photovoltaic, drift, and diffusion currents, β_{ijk} is the photovoltaic tensor, e_j and e^*_k are eigenvectors for light polarization, σ is the total crystal conductivity composed by dark and photoconductivities, and μ_n and μ_p are the mobility of electrons and holes having concentrations n and p, respectively.

According to this model, Eqs. (4) and (5), the thermoelectric effect contributes to the macroscopic space-charge field E_{sc} with a sign linked to the increase or decrease in E_{sc}, depending on polarity of the temperature gradient vector ∇T relative to the spontaneous polarization one P_s. However, this above direct consequence of the model is that exists a contradiction with experimental data when we consider the weak dependence of PRD suppression effect on orientation of the gradient vector ∇T relatively to P_s. Nevertheless, these experimental data are in good accordance with the previously proved conclusion that the macroscopic thermoelectric currents of free carriers play an insignificant role in the macroscopic charge separation, building up E_{sc} in LN.

Finally, we propose the hypothesis that the PRD suppression effect reported here is caused by local thermoelectric currents created by the temperature gradient field, as the light-induced refractive index changes in nominally pure LN arise mainly from local electric fields due to light-induced variations of spontaneous polarization (so-called polarization contribution to the PR effect).[18,19] In contrast this proposal is not valid for iron-doped crystals where macroscopic charge separation gives dominating contribution.

In fact, there are significant differences between the most important features of PR effect in iron-doped and nominally pure LN.[18] For example, according to the usual model of the PR effect, an intensity independent refractive index change is expected. The iron-doped LN samples show the expected intensity independence up to intensity equal to 10^3 W/cm^2. Below this value the spatial index profile is compatible with the model. Moreover, the plateau with steep slopes is typical for the spatial refractive index profiles across a laser beam in iron-doped LN samples. The refractive index change is constant within this plateau, i.e., independent of the laser intensity profile $I(z)$. The refractive index profile generated at same and larger light intensities in nominally pure samples has the anomalous specific characteristics. It is more similar to the laser intensity profile and has no plateau in contradiction to the usual model.[20] Therefore, the local electric field caused by light-induced dipoles within defect sites can be regarded as the dominating contribution to the PR effect in nominally pure crystals.

It has been demonstrated that spatially nonuniform photoexcitation of a pyroelectric crystal containing photoionizable defects generally result in a spatial variation of the macroscopic polarization density.[7,18] The resulting polarization charge density $\rho_p = -\nabla P$ acts as a source for the local electric field that changes the refractive indices and finally influences the PRD.

Trapped electrons (trapped on intrinsic defect sites) modify P in accordance with density of filled traps. In steady state, an equilibrium is established between the field associated with the space-charge density and the $-\nabla P$ polarization charge density. The macroscopic electric field E_{sp} linked to the space charges density ρ_{sp} contributes to P as well through ΔP (space charge) $= (\varepsilon - 1)E_{\mathrm{sp}}$ with ε the dc dielectric constant. In steady state, the total macroscopic electric field from all sources approaches zero. The condition for $E(\mathrm{total}) = 0$ is readily shown to be

$$\nabla(P_+ + P_-) = (\varepsilon - 1)\rho_{\mathrm{sp}}, \tag{6}$$

where P_- is the contribution to P due to filled traps and P_+ is the contribution due to ionized donors.

It has been established[1,3,18,21] that intrinsic antisite defects act as electron traps and donors. If an electron is excited from a defect state to the conduction band, the unit cell dipole moment p_i decreases or increases, depending on to the localization of the defect either on an oxygen site or on Nb (or Li) site, respectively. It is caused by fact that p_i can be regarded as a sum over subcells of the unit cell,

$$p_i = \Sigma Z_{ij} r_{ij}, \tag{7}$$

where Z_{ij} is an effective point charge density and r_{ij} is the center of charge for the jth subcell of unite cell i. The r_{ij} are taken to be the displacements of the jth atom (ion) in the ith unit cell from position in the appropriate centrosymmetric structure, i.e., the paraelectric space group for ferroelectrics.

In real crystals, defects are present and unit cell containing one defect may obviously have a different value for p_i than the perfect one. The macroscopic polarization is then to be computed as

$$P(r) = \Sigma p_i, \tag{8}$$

where the summation is considered over all cells constituting a small volume centered at r. This small volume is chosen so as to contain a statistical quantity of defects, yet to be small in macroscopic terms. Thus, $P(r)$ is a smoothly varying function of position in the crystal and will be locally proportional to the local average density of defects, provided the same coordinates in Eq. (7) for all cells. In LN the oxygen sites contribute with negative value to Eq. (7), while Nb and Li sites contribute positively.[18]

We apply the model developed in Ref. 18, which assumes that a defect exists with the following properties: (1) it is like a double acceptor in that it has three possible charge states (D^+, D^0, and D^-) differing each other by one electronic charge and (2) the site contributes in a positive sense to p_i. Thus the same defect acts as both trap and donor. According to the recently published data,[1,18,22] such an amphoteric defect presents an antisite defect $\mathrm{Nb_{Li}}$ that appears to be in large quantity (concentration of antisite defects is up to 1 mol %) in undoped congruent and near-congruent lithium niobate crystals.

The polarization variation will be proportional to the local difference between densities of D^+ and D^-. Alteration of

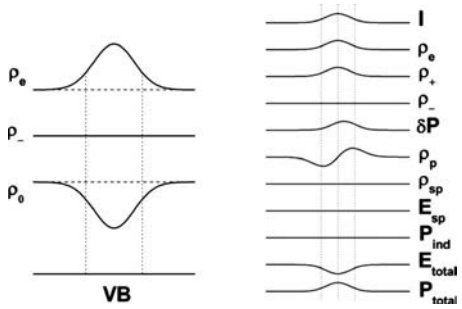

FIG. 10. Distribution of photoexcited carriers ρ_e and schematic of the double-acceptor energy levels ρ_0 and ρ_- after turning on the light (a). Spatial variations (b) at short time after turning on the light of the following: I is light intensity; ρ_e is conduction electrons; ρ_+ is ionized donors; ρ_- is filled acceptors; ∂P is polarization variation from filled and empty traps density variation; ρ_P is polarization charge density; ρ_{sp} is space-charge density; E_{sp} is space-charge field; P_{ind} is polarization induced by space-charge field; E_{tot} is the total electric field from ρ_P and ρ_{sp}; ΔP_{tot} is the total variation in P including both ∂P and P_{ind}.

any Z_{ij} in Eq. (7) by one electronic charge in the lithium niobate structure (with one atom in each subcell and q_i the displacement from the centrosymmetric position), changes p_i by only 8–12%. This provides an upper limit on ΔP corresponding to the fully ionic bonding so that

$$\Delta P(r) < (0.1)(\rho_+ + \rho_-)P_s, \tag{9}$$

where P_s and $\rho_\pm$ are the spontaneous polarization and the relative charged defect densities.

The local increase in densities $\rho_\pm$ is proportional to the intensity distribution of the light. Initially, the density of conduction electrons (ρ_e) and the excess of D^+ sites (ρ_+) varies spatially following the light intensity I. As initially, the carriers have not drifted or diffused over macroscopic distances, polarization variations are also proportional to the light intensity. Thus, variations of the macroscopic polarization and total electric field are both Gaussian, with the same spatial dependence as the light intensity, as shown in Fig. 10.

For lithium niobate, the field-based electro-optic effect description is appropriate for externally applied fields, but internal electro-optic effects must be described in terms of polarization rather than field.[18] So we can write for ordinary and extraordinary refractive index changes

$$\Delta n_e = -(n_e^3/2)[r_{33}\Delta P/(\varepsilon_{33}-1)],$$

$$\Delta n_o = -(n_o^3/2)[r_{13}\Delta P/(\varepsilon_{33}-1)], \tag{10}$$

where r_{13} and r_{33} are the clamped electro-optic coefficients.

For congruent LN crystals,

$$\delta(n_e - n_o) = -(0.645 - 0.138)\Delta P \tag{11}$$

with ΔP in C/m^2, or since $P_s = 0.71\ C/m^2$,[7]

$$\delta(n_e - n_o) = -A(\Delta P/P_s). \tag{12}$$

Accordingly, from data on maximum PR effect magnitude in LN (Ref. 4) with $\delta(n_e - n_o)$ equal to 10^{-3}, $\Delta P/P_s$ must be $\sim 3\times 10^{-3}$. If the change in the cell dipole moment between cells containing D^+ and D^- defects is of the order of 5% of the perfect cell moment,[18] i.e., the half of the maximum ionic bonding amount, then at least, 1% of the unit cells must contain an ionizable defect. It is very important to note that this amount deduced by our analysis coincides exactly with the recently published data on concentration of antisite Nb_{Li} defects in undoped congruently melting lithium niobate crystals.[1,4,18,22]

Within the consideration of the crystal stoichiometry, the limited range over which the Nb content may be increased suggests that Czochralski-grown crystals cannot be substantially improved in the PRD-resistant direction. A macroscopically averaged [Li]/[Nb] ratio of unity or greater does not guarantee the absence of Nb excess stacking faults but only, that Li-rich faults must be present in a compensating extent.[1,18] Improvement in damage-resistant direction thus requires growth of microscopically stoichiometric material, i.e., reduction in the absolute density of defects. Thus, the finding mentioned above allows to explain the absence of the close correlation between PRD magnitude and [Li]/[Nb] ratio averaged over a certain crystal (see Tables I and II).

No structural defects are created in the crystal by low-intensity light illumination, thus we need to consider only two possibilities: excitation of bipolarons and excitation of hole polarons. A bipolaron consists of a $Nb^{4+}{}_{Li}$ polaron occupying a Li lattice site and a $Nb^{4+}{}_{Nb}$ polaron occupying a regular Nb lattice site, coupled by the induced lattice distortion, forming a diamagnetic system with antiparallel spins.[1,22] Upon creation or decay of bipolarons, one would thus expect to observe single $Nb^{4+}{}_{Li}$ and $Nb^{4+}{}_{Nb}$ polarons. Furthermore, the nonlinear absorption α_{li} in $LiNbO_3$:Fe and in undoped lithium niobate demonstrates the generation of holes in the valence band by two-photon band to band transitions.[23] They are not annihilated and can move to a pinning center. Thus, it was concluded,[23] that the long-lived light-induced effects might be caused by small bound O^- polarons, i.e., one hole trapped by an oxygen ion near a lithium vacancy. In case of photogeneration of polarons, electrons are excited by two-photon excitations, leaving holes in the valence band. These electrons form $Nb^{4+}{}_{Li}$ polarons. Holes are trapped by O^{2-} near lithium vacancies, forming O^- hole polarons. Small polarons decay into empty traps and they recombine afterwards with hole polarons. They recombine on longer time in the few seconds scale. The dependence of the recombination rate on the number of $Nb^{4+}{}_{Li}$ polarons opens the door to a manipulation of the polaron lifetimes by changing the $Nb^{4+}{}_{Li}/Nb^{5+}{}_{Li}$ ratio via a reduction/oxidation treatment.[23]

Mentioned above findings allow to suggest that the D^-, D^0, and D^+ defects in our model, Eqs. (8)–(11), are related to small $Nb^{4+}{}_{Li}$ (single, or forming bipolarons) and O^- hole polarons. It should be noted that significant concentration ($\geq 10^{19}$ cm^{-3}) of bipolarons exists even in slightly reduced nominally pure crystals.[4,17] At the same time, all nominally pure lithium niobate samples fabricated with standard conditions may be regarded as slightly reduced crystals.[4]

We interpret the results on suppression of PRD via temperature gradient as implying a threshold value of temperature gradient, ∇T, where local thermoelectric current of photoexcited carriers, appearing due to microscopic carriers drift over a distance comparable with a unit cell size, can induce spatial redistribution of filled polaron states. This redistribu-

tion is accompanied by instant recombination of small and hole polarons, i.e., depletion in local difference of the densities $\rho_{\pm}$ and, thus, a disappearance of macroscopic polarization variations within illuminated area. Such a drift can be explained by the internal-field model of PRD,[24] assuming that a ∇T-induced increment of the internal field is the driving force of the local drift of carriers. Therefore, this threshold value ∇T_{th} can be roughly estimated by

$$e\rho_{+} + g(dI/dz) = \nabla T_{\text{th}}(dP/dT), \tag{13}$$

where g is the product of photoexcitation quantum efficiency, absorption coefficient, and electron charge, dI/dz is the light-intensity distribution along beam cross section, and $e\rho_{+}$ is the effective charge density associated with empty traps, i.e., with D^{+} intrinsic defects related to allowed ground-polaron state in bandgap. In notations D^{+} and ρ_{+}, we use the formal charge only as a convenient label to denote the charge environment of the atom in question.

Note that Eq. (13) has been obtained in frame of "plasma" model, describing the direct contribution of free electrons to refractive index change.[11] Similar to general conclusion of Ref. 11, our experimental results do not support this model. Thus, we use Eq. (13) in formal sense only, to describe the specific equilibrium state of charge transfer process.

It means that $\Delta P=0$ at $\nabla T \geq \nabla T_{\text{th}}$, i.e., according to Eqs. (10)–(12), light-induced refractive index changes disappear. According to Ref. 11, the dependence of densities profiles $\rho_{\pm}(z)$ on temperature gradient ∇T and light-intensity profile $I(z)$ can be described by second-order differential equation. In general, this equation is not tractable and, therefore, we use Eq. (13) to describe only the particular case mentioned above. Equation (13) is not valid in case of marked macroscopic charge separation, when the space-charge field gives a significant or dominating contribution in the refractive index modulation, Fig. 11. An insignificant space-charge field contribution to the apparent steady-state PRD observed at low and moderate intensities of the red light (632.8 nm) can be explained by the greatly reduced rate at which electrons drift out of illuminated region and the weak thermal re-excitation of trapped electrons in the proximity of this region.[24]

Taking the density of polarons equal to 1.7×10^{19} cm^{-3} generated by a high-intensity (4×10^{8} W/cm^{2}) laser pulses at 532 nm in crystal and with a linear absorption coefficient around 5 cm^{-1},[23] one can estimate the threshold value ∇T_{th} in the order of 10^{2} K/cm. This rough estimation, performed via Eq. (13), considers the real small values of the linear absorption coefficient (see Table I), the low-intensity excitation regime ($\leq 2 \times 10^{3}$ W/cm^{2}) at 632.8 nm, the spectral dependences[16] of absorption cross section of polarons and bipolarons, and (dP/dT) to be equal of the pyroelectric coefficient defined after Eq. (3). Thus, this theoretical estimation result is in quite satisfactory agreement with our experimental data presented above (see Table II). By the way, further studies are required to develop an exact quantitative model.

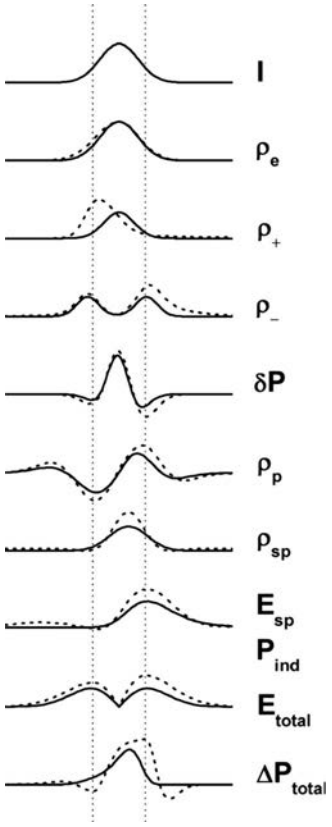

FIG. 11. Spatial variation of the quantities shown in Fig. 10 for a nominally pure crystal after high-intensity long-term exposure at uniform temperature gradient (solid curves) and iron-doped crystals for both intermediate and long-term exposure (dashed curves).

V. SUMMARY

The total suppression of PRD is possible to reach in nominally pure LN crystals with aid of transverse steady-state temperature gradient ∇T, above a specific threshold ∇T_{th}. Such a specific threshold can be controlled by extra reduction/oxidation annealing, as ∇T_{th} decreases with the increase in bipolaron absorption band, which is largely affected by this extra annealing. It has been demonstrated that small threshold ∇T_{th} (≤ 41 K/cm) could be achieved at low (practically acceptable) level of optical absorption (≤ 0.16 cm^{-1}). However, the full suppression of PRD is not available for stable long-term operation in the range of days. Despite this drawback, the partial suppression of PRD via temperature gradient has great practical importance, as inherent residual PRD is smaller than maximum acceptable levels required in many applications.

Main advantages of this method of PRD suppression consist of its relative technical simplicity and of its possibility to select any operational or functioning temperature values within a local area, e.g., within the waist of the focused laser beam. The latter is one of the most important task for nonlinear optical converters, where a specific temperature have to be fixed to obtain exact phase matching conditions.

It was found that there is a clear correlation between PRD magnitude and modulation depth of the corresponding Z-scan trace either for the various samples at fixed values of ∇T, or for the data obtained at different ∇T for a given crys-

tal. Thus, *Z*-scan measurements can be used as well to compare the PRD suppression effect in various crystals since the peak-valley configuration of the *Z*-scan trace distinguishes clearly samples above and below ∇T_{th}, which can be regarded as a specific functional parameter of each crystal.

The theoretical explanation of the PRD suppression effect is given on basis of the so-called polarization field model. We have demonstrated that light-induced refractive index changes caused by local variations of the spontaneous polarization due to photoionization of the intrinsic defects in LN crystals can be erased by a local thermoelectric current of light-induced charge carriers (polarons, bipolarons, and hole polarons) induced by a steady-state temperature gradient. At the same time, such a gradient-induced local current cannot erase the light-induced refractive index change created by macroscopic charge separation. This prediction of our theoretical model is confirmed by fact that no any PRD suppression (even partial) has been observed in iron-doped ($[\mathrm{Fe}] \geq 0.01$ wt %) lithium niobate crystals at relatively small temperature gradients used in this study.

[1]O. F. Schirmer, O. Thiemann, and M. Wöhlecke, J. Phys. Chem. Solids **52**, 185 (1991).
[2]G. Kh. Kitaeva, K. A. Kuznetsov, V. F. Morozova, I. I. Naumova, A. N. Penin, A. V. Shepelev, A. V. Viskovatich, and D. M. Zhigunov, Appl. Phys. B: Lasers Opt. **78**, 759 (2004).
[3]K. Buse, Appl. Phys. B: Lasers Opt. **64**, 391 (1997).
[4]S. M. Kostritskii and O. G. Sevostyanov, Appl. Phys. B: Lasers Opt. **65**, 527 (1997).
[5]G. I. Malovichko, V. G. Grachev, E. P. Kokanyan, O. F. Schirmer, K. Betzler, B. Gather, F. Jermann, S. Klauer, U. Schlarb, and M. Wöhlecke, Appl. Phys. A: Solids Surf. **A56**, 103 (1993).
[6]E. E. Robertson, R. W. Eason, Y. Yokoo, and P. J. Chandler, Appl. Phys. Lett. **70**, 2094 (1997).
[7]A. M. Prokhorov and Yu. S. Kuz'minov, *Physics and Chemistry of Crystalline Lithium Niobate* (Adam Hilger, Bristol, 1990).
[8]V. A. Pashkov, N. M. Solov'eva, and N. B. Angert, Fiz. Tverd. Tela (Leningrad) **21**, 92 (1979).
[9]L. B. Schein, P. J. Cressman, and L. E. Cross, J. Appl. Phys. **49**, 798 (1978).
[10]L. B. Schein, P. J. Cressman, and F. M. Tesche, J. Appl. Phys. **48**, 4844 (1977).
[11]L. G. Reznik, A. A. Anikiev, B. S. Umarov, and J. F. Scott, Ferroelectrics **64**, 215 (1985).
[12]S. Bian, Opt. Commun. **141**, 292 (1997).
[13]L. Pálfalvi, G. Almási, J. Hebling, Á. Péter, and K. Polgár, Appl. Phys. Lett. **93**, 902 (2004).
[14]L. Pálfalvi, G. Almási, J. Hebling, Á. Péter, and K. Polgár, CLEO'2002, 12–17 May, 2002, Long Beach, California, USA, 2002 (unpublished).
[15]S. Bian, J. Frejlich, and K. H. Ringhofer, Phys. Rev. Lett. **78**, 4035 (1997).
[16]F. Jermann, M. Simon, R. Bower, E. Kratzig, and O. F. Schirmer, Ferroelectrics **165**, 319 (1995).
[17]A. Dhar and A. Mansingh, J. Appl. Phys. **68**, 5804 (1990).
[18]W. D. Johnston, Jr., J. Appl. Phys. **41**, 3279 (1970).
[19]L. Wan, Y. Yuan, and G. Assanto, Opt. Commun. **74**, 361 (1990).
[20]O. Althoff and E. Kratzig, Proc. SPIE **1273**, 12 (1990).
[21]F. Jermann and J. Otten, J. Opt. Soc. Am. B **10**, 2085 (1993).
[22]H. Muller and O. F. Schirmer, Ferroelectrics **125**, 319 (1992).
[23]P. Herth, T. Granzow, D. Schaniel, Th. Woike, M. Imlau, and E. Kratzig, Phys. Rev. Lett. **95**, 067404 (2005).
[24]F. S. Chen, J. Appl. Phys. **40**, 3389 (1969).